Evidence of Two-Gap s-Wave Superconductivity in $YBa_2Cu_3O_{7-x}$ from Microwave Surface Impedance Measurements

N. Klein, N. Tellmann, H. Schulz, and K. Urban
Institut für Festkörperforschung, Forschungszentrum Jülich GmbH, D-52425 Jülich, Germany

S. A. Wolf
Naval Research Laboratory, Washington D.C. 20375-5000

V. Z. Kresin
Lawrence Berkeley Laboratory, University of California, Berkeley, California 94720
(Received 8 July 1993)

Epitaxial thin films of $YBa_2Cu_3O_{7-x}$ with low cation and oxygen disorder exhibit two features in the temperature dependence of the microwave surface impedance which are consistent with a weak s-wave superconducting state associated with the CuO chains. First, both the microwave surface resistance and the magnetic field penetration depth exhibit a weak exponential temperature dependence below 30 K corresponding to an energy gap of about 6 meV. Second, the penetration depth exhibits a small bump at about 60 K, which is consistent with a two-band BCS calculation using 6 meV for the smaller gap.

PACS numbers: 74.25.Nf, 74.72.Bk, 74.76.Bz

The question about the pairing mechanism in high-temperature superconducting cuprates is still under discussion [1]. Key experiments to rule out or to support different theories are those which provide information on the anisotropy of the energy gap, especially concerning the question of nodes in the gap. Since photoemission, tunneling, and Raman studies have not yet answered this question unambiguously, the promise resides on precise measurements of the temperature dependence of both the microwave surface resistance R_s and the penetration depth of the magnetic field λ. In particular, the occurrence of an exponential temperature dependence can rule out d-wave theories.

However, due to the short coherence length in the cuprates the microwave surface impedance can be strongly affected by impurity phases and granularity arising from the Josephson-contact behavior of grain boundaries. To date, the temperature dependence of the surface impedance only reflects intrinsic properties for some high quality epitaxial thin films and bulk single crystals of the $RBa_2Cu_3O_{7-x}$ (R = rare earth) compounds, which exhibit low R_s values for temperatures approaching zero [2].

One peculiarity of $RBa_2Cu_3O_{7-x}$ arises from the CuO chains. There is evidence from optical [3] and far infrared [4] reflectivity as well as from dc resistivity [5] measurements on detwinned bulk single crystals of $YBa_2Cu_3O_{7-x}$ that the chains are conducting. According to theoretical investigations by Kresin and Wolf [6–8], superconductivity can be induced in the chains from the CuO_2 planes by the internal proximity effect and phonon-mediated charge transfer. The energy gap of the induced superconducting chain state is predicted to be smaller than the energy gap of the planes. Double gap structures in $YBa_2Cu_3O_{7-x}$ have indeed been observed in tunneling experiments, but not very reproducibly [9]. Recently, a pronounced double gap structure without zero bias conductance was observed in bulk single crystal break junctions of $YBa_2Cu_3O_{7-x}$ [10]. The first evidence of the existence of a small gap in $YBa_2Cu_3O_{7-x}$ associated with CuO chains came from nuclear magnetic resonance experiments [11,12]. Furthermore, as a method to probe the density of thermal quasiparticle excitations, measurements of the microwave surface resistance of epitaxial thin films prepared by high oxygen pressure sputtering [13–15] or by coevaporation [16] showed strong evidence of a small energy gap associated with the CuO chains. For the films prepared by sputtering the observed weak exponential $R_s(T)$ behavior below about $T_c/2$ was found to be accompanied by a nonlinearity of the dc resistivity $\rho(T)$ with $d^2\rho/dT^2 < 0$ [13,14]. Experiments on detwinned single crystals indicated that nonlinear $\rho(T)$ behavior is associated with the CuO chains [5]. Upon oxygen depletion, the exponential $R_s(T)$ dependence [15] and the nonlinear $\rho(T)$ dependence [17] disappear. For oxygen-deficient films, an increase of R_s with oxygen disorder was observed [15,18]. This shows that the CuO chains have a strong influence on the microwave losses. In particular, the suppression of exponential behavior upon oxygen depletion is consistent with the prediction that in oxygen-deficient $YBa_2Cu_3O_{7-x}$ the induced superconducting state is destroyed by magnetic pair breaking [6–8].

Data on $\lambda(T)$ at low temperatures do not yet show consistent behavior. Anlage *et al.* [19] reported a weak exponential temperature dependence, whereas Beasley *et al.* found good agreement with T^2, except for small deviations below 10 K [20,21]. In contradiction to these results a linear temperature dependence was reported recently by Hardy *et al.* [22] and interpreted by the authors as an indication of d-wave superconductivity. At higher temperatures, however, the $\lambda(T)$ data are highly consistent with s-wave behavior [23].

0031-9007/93/71(20)/3355(4)$06.00

In the present contribution we report both on surface resistance and penetration depth measurements on $YBa_2Cu_3O_{7-x}$ films prepared by high oxygen pressure sputtering. The results show a consistent picture of two gap s-wave superconductivity with a small energy gap Δ of approximately 6 meV.

Several c-axis oriented 1×1 cm^2 $YBa_2Cu_3O_{7-x}$ films of 250 nm thickness were prepared by high oxygen pressure dc sputtering either on single crystalline (001) oriented $LaAlO_3$ or on (110) oriented $NdGaO_3$ substrates. The preparation technique and the general structural and electrical transport properties of the films were discussed elsewhere [13]. It should be emphasized that in contrast to other deposition techniques a high oxygen pressure of about 3 mbar is applied during deposition. The c-axis lattice parameter, as determined by x-ray diffractometry, was found to be 1.167 nm, in agreement with values measured for fully oxygenated bulk samples [24]. The films exhibit a high degree of crystalline perfection, as, e.g., indicated by a typically 1.2° half-width of the rocking curves of the (001) peaks in x-ray diffraction [13].

The microwave surface impedance $Z_s(T)=R_s(T)+i\omega\mu_0\lambda(T)$ ($\omega=2\pi f$, $\mu_0=1.256\times10^{-6}$ Vs/Am) at 18.9 GHz was determined by recording the resonant frequency f and the quality factor of a shielded dielectric sapphire resonator with one endplate of the shielding cavity partially replaced by the film under investigation [14]. To account for losses in the copper walls and thermal expansion of the cavity, calibration measurements with copper and niobium samples were performed as described in Ref. [14]. In particular, due to the low thermal expansion of sapphire below 20 K the thermal expansion effect was found to be negligible within our measuring accuracy of ±0.2 nm for changes of the penetration depth $\Delta\lambda$ with temperature. Within these errors, changes of the resonant frequency Δf are related to $\Delta\lambda$ by

$$\Delta f=\frac{\pi\mu_0 f^2\Delta\lambda}{G}\left(\coth[d/\lambda(0)]+\frac{d/\lambda(0)}{\sinh^2[d/\lambda(0)]}\right). \quad (1)$$

The expression in large parentheses accounts for a redistribution of the high-frequency current resulting from the finite film thickness d [25]. In the temperature range below about 30 K, the temperature dependence of this bracketed expression caused by the temperature dependence of λ can be neglected. G is a geometric factor which is 830 Ω for our cavity and $\lambda(0)$ is the absolute value of $\lambda(T)$ at the temperature where $\Delta\lambda$ is put to zero. Since with our resonator technique only relative values of λ can be measured, $\lambda(0)$ was determined by a fit of a theoretical temperature dependence to the $\lambda(T)$ data. For the absolute value of the surface resistance there is a systematic error of ±50 $\mu\Omega$ due to the subtraction of the losses in the cavity walls. Changes of R_s with temperature can be measured with an accuracy of ±10 $\mu\Omega$ for $R_s\leq4\times10^{-4}$ Ω.

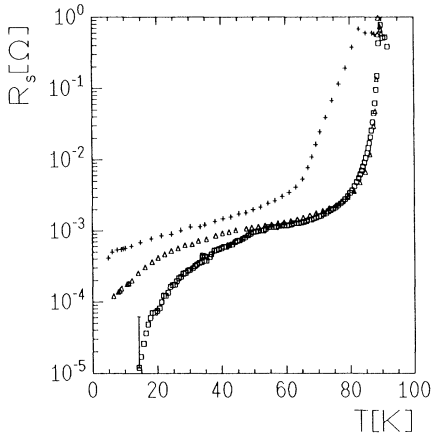

FIG. 1. Surface resistance versus temperature measured at 18.9 GHz for two fully oxygenated $YBa_2Cu_3O_{7-x}$ films on $NdGaO_3$ (squares) and $LaAlO_3$ (triangles) and an oxygen-deficient film on $LaAlO_3$ (crosses) with $x\approx0.2$.

Figure 1 shows the surface resistance versus temperature for two fully oxygenated $YBa_2Cu_3O_{7-x}$ films on $NdGaO_3$ (squares) and $LaAlO_3$ (triangles) and for an oxygen-deficient film on $LaAlO_3$ (crosses) with $x\approx0.2$, as determined from the c-axis lattice parameter [24]. The two fully oxygenated samples indicate the typical variation in the temperature dependence of R_s, which was observed reproducibly for about 30 films prepared under the same conditions. We found a tendency for the films on $NdGaO_3$ to exhibit the stronger low-temperature decrease of $R_s(T)$. This is presumably due to a higher crystalline quality of the films, in particular at the substrate-film interface.

Figure 2 shows the low temperature region of R_s plot-

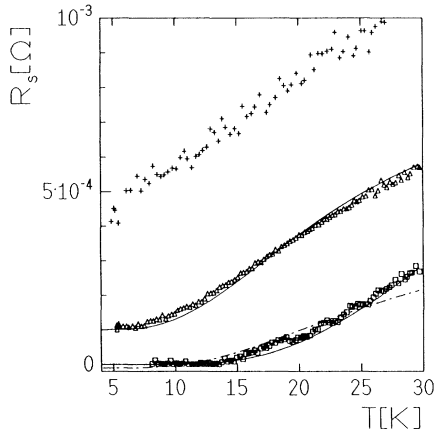

FIG. 2. Linear plot of the low temperature region of the surface resistance for the films from Fig. 1. The solid and dash-dotted lines are fits of Eq. (2) to the data (squares and triangles).

ted linearly against temperature. The solid and dash-dotted lines represent fits of the analytical low temperature approximation from BCS theory [26]

$$R_s(\omega,T)=\frac{1}{2}\omega^2\mu_0^2\lambda^3\sigma_{1,n}\frac{2\Delta}{kT}\ln\left(\frac{\Delta}{\hbar\omega}\right)\exp(-\Delta/kT)\times\left[\coth[d/\lambda(0)]+\frac{d/\lambda(0)}{\sinh^2[d/\lambda(0)]}\right], \quad (2)$$

using $\lambda(0)=134$ nm from the calculated $\lambda(T)$ curves (see next section), $\hbar=1.0546\times10^{-34}$ Js, and $k=1.3807\times10^{-23}$ J/K. The value of the normal state conductivity $\sigma_{1,n}$ and the energy gap Δ were used as fit parameters. For the films on $LaAlO_3$ and $NdGaO_3$ the best fits (solid lines) were obtained with $\Delta=5$ meV, $\sigma_{1,n}=4.5\times10^5$ $(\Omega\,\mathrm{cm})^{-1}$ and $\Delta=10$ meV, $\sigma_{1,n}=8\times10^5$ $(\Omega\,\mathrm{cm})^{-1}$, respectively. For the film on $LaAlO_3$ a temperature-independent surface resistance of 100 $\mu\Omega$ has to be added to Eq. (1) to obtain an appropriate fit. As indicated by the dash-dotted line, Δ values as low as 6 meV [$\sigma_{1,n}=2.5\times10^5(\Omega\,\mathrm{cm})^{-1}$] can also fit $R_s(T)$ of the film on $NdGaO_3$ up to 25 K. Such a discrepancy may be due to a temperature dependence of $\sigma_{1,n}$ resulting from a temperature-dependent quasiparticle scattering rate [27]. Moreover, it may explain the fact that the $\sigma_{1,n}$ values obtained from the fit are significantly above the normal state value of 2×10^4 $(\Omega\,\mathrm{cm})^{-1}$ measured at 100 K. In contrast to the fully oxygenated films, the oxygen-deficient films exhibit a linear temperature dependence and a significantly higher level of R_s.

Figure 3 shows $\lambda(T)$ for the films where $R_s(T)$ was depicted in Figs. 1 and 2. One feature which appears in all films with exponential $R_s(T)$ behavior is a small bump at about 60 K. This feature can be explained by assuming two conducting subsystems (labeled a and b), which are arranged in thin (on the scale of the penetration depth) alternating layers being oriented in the direction of the high frequency currents. This corresponds to parallel currents through both subsystems, i.e., the conductivities have to be added. In the case of local electrodynamics, the imaginary part of the conductivity is proportional to $1/\lambda^2$:

$$\frac{1}{\lambda^2(T)}=\frac{1}{\lambda_a(T)^2}+\frac{1}{\lambda_b(T)^2}, \quad (3)$$

with

$$\frac{1}{\lambda_{a,b}(T)}=\frac{1}{\lambda_{a,b}(0)}\left[1-2\int_{\Delta_{a,b}(T)}^{\infty}-\frac{\partial f(\epsilon)}{\partial\epsilon}\frac{\epsilon}{\sqrt{\epsilon^2-\Delta_{a,b}(T)^2}}d\epsilon\right]$$

and

$$f(\epsilon)=\frac{1}{\exp(\epsilon/kT)+1}.$$

Using the temperature dependence of $\lambda_{a/b}$ from BCS theory [26], it becomes obvious that this bump is a strong indication of the existence of two separate subsystems with different gap values. In the frame of the model of induced superconductivity [6–8], the presence of two gaps means that the density of states $N(\epsilon)$ for both subsystems (CuO_2 planes and the CuO chains) has two distinct peaks at $\epsilon=\Delta_a$ and $\epsilon=\Delta_b$. Therefore Eq. (3) can only describe the general shape of the $\lambda(T)$ curves in a two-gap system. More realistic calculations in the frame of the induced superconductivity model taking into account calculated densities of states, strong coupling corrections as well as corrections due to the high frequency of the electromagnetic field are in progress.

The solid and dash-dotted lines in Fig. 3 represent a calculation of $\lambda(T)\coth[d/\lambda(T)]$ with $\lambda(T)$ from Eq. (3) using $T_c=89$ K, $\lambda_a(0)=240$ nm, and $\lambda_b(0)=165$ nm corresponding to plasma energies $E_p=\hbar c/\lambda=E_{p,t}=(E_{p,a}^2+E_{p,b}^2)^{0.5}=1.45$ eV for the total and $E_{p,b}=1.2$ eV for the charge carrier density in the b phase. Similar values have been found in normal state optical reflectivity measurements on detwinned bulk single crystals for the crystallographic a direction (CuO_2 planes and CuO chains, corresponding to $E_{p,t}$) and b direction (CuO chains, corresponding to $E_{p,b}$) [3]. For $\lambda(0)$ a value of 136 nm results from the calculation, which represents an appropriate fit to the $\lambda(T)$ data of both fully oxygenated films. For the energy gaps $\Delta_a(0)=25$ meV and $\Delta_b(0)=6$ (solid line) and 10 meV (dash-dotted line) and for $\Delta_{a/b}(T)/\Delta_{a/b}(0)$ values tabulated by Mühlschlegel [28] were used. The calculated curves in Fig. 3 show that the position of the bump is strongly affected by $\Delta_b(0)$. For the oxygen-deficient film, however, no bump was observed. Therefore our results are consistent with a two-gap system with a small gap of about 6 meV associated with the CuO chains. According to Ref. [29], small bumps in $\lambda(T)$ were also observed in cavity experiments for films prepared by laser ablation and sputtering. Moreover, in Ref. [19] a tendency to strong (weak) coupling behavior in the high (low) temperature regime of $\lambda(T)$ was reported. This is consistent with our data taking into account a possible smearing of the peak in the

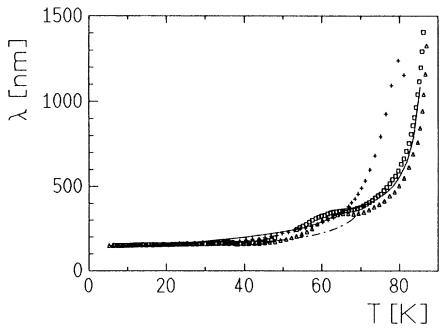

FIG. 3. $\lambda(T)$ for the films from Fig. 1. The solid and dash-dotted lines represent calculations according to Eq. (3) using values of 6 and 10 meV for the small energy gap.

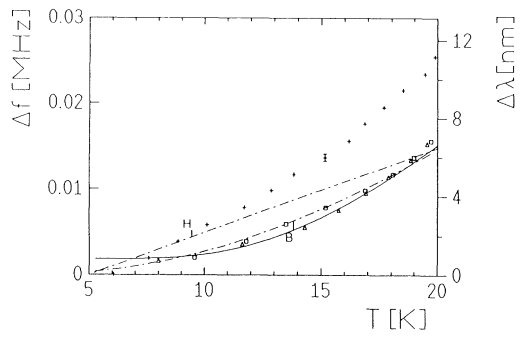

FIG. 4. $\Delta f(T)$ and $\Delta\lambda(T)$ for the films from Fig. 1. The solid line represents a fit of Eq. (4) to the data (squares and triangles). Moreover, literature data from Beasley [20] (dash-dotted line, labeled B) and Hardy *et al.* [22] (dash-dotted line, labeled H) are included.

density of states at $\epsilon=\Delta_b$ due to disordering.

Finally, the low temperature behavior of $\lambda(T)$ was investigated. Figure 4 shows $\Delta f(T)$ and $\Delta\lambda(T)$ as well as a fit according to the low temperature approximation from BCS theory [26] (solid line) using Δ as a fit parameter and $\lambda(0)$, $E_{p,t}$, and $E_{p,b}$ as determined in the previous section:

$$\Delta\lambda(T)=\lambda(0)\left[\frac{E_{p,b}}{E_{p,t}}\right]^2\sqrt{\pi\Delta/2kT}\exp(-\Delta/kT). \quad (4)$$

It is important to note that the plasma energies of chains and planes enter this equation to account for the charge carriers in the planes. The exponential temperature dependence resulting from the large gap, however, has no significant influence on the temperature dependence of $\Delta\lambda$ below 20 K. Figure 4 shows that our experimental data on the fully oxygenated films are consistent with Eq. (4) using $\Delta=6$ meV. Moreover, Beasley's data on films prepared by off-axis sputtering [20] (dash-dotted line, labeled B) also show a tendency to weak exponential behavior, in contrast to Hardy's [22] data on bulk single crystals (dash-dotted line, labeled H). The oxygen-deficient film, however, exhibits the largest slope and an almost quadratic temperature dependence. We speculate that the linear temperature dependence observed by Hardy *et al.* is due to the fact that the single crystals may not be uniformly oxygenated. This can also explain its high residual losses reported by Bonn *et al.* [27].

In conclusion, our microwave surface impedance data show a consistent picture of two-band s-wave superconductivity in fully oxygenated $YBa_2Cu_3O_{7-x}$ films with low cation disorder. Moreover, our data indicate that the temperature dependence of both the surface resistance and the penetration depth are consistent with an energy gap Δ of approximately 6 meV corresponding to $2\Delta/kT_c\approx 1.6$. Upon oxygen depletion the s-wave temperature dependence of the surface impedance disappears. These observations are consistent with an induced superconducting state in the CuO chains of $YBa_2Cu_3O_{7-x}$

This work was funded in part by the German consortium First Applications of High Temperature Superconductors in Micro- and Cryoelectronics. V. Z. Kresin's research is supported by ONR under Contract No. DE-AC03-76S-F00098.

[1] Barbara Goss Levi, Phys. Today **46**, No. 5, 17 (1993).
[2] N. Klein, Mater. Sci. Forum. **130-132**, 373 (1993).
[3] A. Zibold *et al.*, Appl. Phys. Lett. **61**, 345 (1992).
[4] Z. Schlesinger *et al.*, Physica (Amsterdam) **185-189C**, 57 (1991).
[5] T. A. Friedmann *et al.*, Phys. Rev. B **42**, 6217 (1990).
[6] V. Z. Kresin and S. A. Wolf, Physica (Amsterdam) **198C**, 328 (1992).
[7] A. Andreone, V. Z. Kresin, and S. A. Wolf, J. Supercond. **5**, 339 (1992).
[8] V. Z. Kresin and S. A. Wolf, Phys. Rev. B **46**, 6458 (1992).
[9] J. M. Valles *et al.*, Phys. Rev. B **44**, 11986 (1991).
[10] B. A. Aminov *et al.*, J. Supercond. (to be published).
[11] W. W. Warren *et al.*, Phys. Rev. Lett. **59**, 1860 (1987).
[12] S. E. Barrett *et al.*, Phys. Rev. B **41**, 6283 (1990).
[13] U. Poppe *et al.*, J. Appl. Phys. **71**, 5572 (1992).
[14] N. Klein *et al.*, J. Supercond. **5**, 195 (1992).
[15] N. Klein *et al.*, IEEE Trans. Appl. Supercond. **3**, 1102 (1993).
[16] A. Gladun *et al.*, Cryogenics **32**, 1071 (1992).
[17] M. I. Faley *et al.*, IEEE Trans. Appl. Supercond. **3**, 1082 (1993).
[18] S. Orbach *et al.*, J. Alloys Compounds **195**, 555 (1993).
[19] S. M. Anlage *et al.*, Phys. Rev. B **44**, 9764 (1991).
[20] M. R. Beasley, Physica (Amsterdam) **209C**, 43 (1993).
[21] Zhengxiang Ma *et al.*, Phys. Rev. Lett. **71**, 781 (1993).
[22] W. N. Hardy *et al.*, Phys. Rev. Lett. **70**, 3999 (1993).
[23] B. Batlogg, Phys. Today **44**, No. 6, 44 (1991).
[24] J. D. Jorgensen *et al.*, Phys. Rev. B **41**, 1863 (1990).
[25] N. Klein *et al.*, J. Appl. Phys. **67**, 6940 (1990).
[26] J. P. Turneaure, J. Halbritter, and H. A. Schwettman J. Supercond. **4**, 341 (1991).
[27] D. A. Bonn *et al.*, Phys. Rev. B **47**, 11314 (1993).
[28] B. Mühlschlegel, Z. Phys. **155**, 313 (1959).
[29] S. Orbach, University of Wuppertal (private communication).